Ferrite-damped higher-order mode study in the Brookhaven energy-recovery linac cavity

H. Hahn, E. M. Choi, and L. Hammons
Collider-Accelerator Department, Brookhaven National Laboratory, Upton, New York 11973-5000, USA
(Received 6 November 2008; published 27 February 2009)

A superconducting energy-recovery linac (ERL) is under construction at Brookhaven National Laboratory (BNL) to serve as a test bed for an application to upgrades of the Relativistic Heavy Ion Collider (RHIC). The damping of higher-order modes in the superconducting five-cell cavity is of paramount importance and represents the topic of this paper. Achieving the damping by the exclusive use of two ferrite absorbers and the adoption of a space-saving step instead of the conventional taper are part of the exploratory study. Absorber properties which are portable to simulation programs for the ERL cavity have been obtained by measuring the absorber as a ferrite-loaded pill-box cavity. Measured and simulated results for the lowest dipole modes in the prototype copper cavity with one absorber are discussed. First room-temperature measurements of the fully assembled niobium cavity string are presented which confirm the effective damping of higher-order modes by the ferrite absorbers, and which give credibility to the simulated R over Q's in the ERL.

DOI: 10.1103/PhysRevSTAB.12.021002 PACS numbers: 29.20.−c, 41.20.−q

I. INTRODUCTION

A superconducting energy-recovery linac (ERL) is under construction at Brookhaven National Laboratory (BNL) to investigate concepts for electron cooling of ions and coherent electron cooling of high-energy protons in the Relativistic Heavy Ion Collider (RHIC), or for an envisioned electron-ion collider [1,2]. The ERL test facility is based on a niobium superconducting (SC) 703.75 MHz five-cell cavity capable of accelerating electrons to 20 MeV and a SC 2.5 MV electron gun. Operation of the ERL is planned in the high-current mode with 0.5 A/0.7 nC per bunch at ~703 MHz, or in the high-charge mode with 5 nC at 10 MHz. Achieving these goals depends on damping of higher-order modes (HOMs) in the SC ERL cavity. Providing the possibility of damping and avoiding any trapped HOMs was the basic objective in the design of the five-cell cavity [3–5]. The design followed the techniques developed at Cornell [6,7] and KEKB [8] for ferrite absorbers, which lead to a cavity design with comparatively large iris apertures allowing propagation of HOMs to the external absorber. However, the exclusive use of ferrite absorbers for a multicell cavity and the space-constrained replacement of tapered end sections by steps set the Brookhaven ERL apart from the other projects.

The five-cell cavity was designed by BNL, the niobium structures and cryomodules were fabricated by AES on Long Island [9], the ferrite absorbers were fabricated according to Cornell-print by ACCEL in Germany [10], and the cavity was processed at the Thomas Jefferson National Accelerator Facility. The ERL cavity has been delivered, and the cavity string assembled in its helium vessel with the thermal isolation sections and the ferrite absorber is shown in Fig. 1.

This paper is focused on the experimental and computational study of damping the dominant lower-frequency dipole modes in the ERL cavity by the ferrite absorber. The determination of the HOM damping is done by comparing forward scattering coefficient (S_{21}) network analyzer measurements with simulations using the CST Microwave Studio (MWS) program [11]. Preceding the final design and fabrication of the Nb cavity a prototype five-cell Cu cavity was fabricated and for the present study a MWS model of the bare ERL cavity was constructed based on the detailed AES fabrication drawings. In order to establish a reference basis, global damping measurements of the Cu cavity with one prototype absorber were performed yielding the results given in Sec. II. The major objective of the subsequent R&D work was to obtain quantitative R/Q and shunt impedance values for the ERL cavity with all its attachments assembled. A necessary intermediate step consisted in determining ferrite absorber properties in a form that is portable into the MWS program for simulation of the ERL and other relevant cavities. This task was addressed by investigating several compact ferrite-loaded pill-box cavities [12–14] with summary results given in Sec. III.

The access to the ERL cavity prior to assembly in its cryostat represented an excellent opportunity to collect new data. Making tests directly on the cavity provided the first definite results for the ERL HOMs. The ERL string differs from the prototype cavity primarily by the presence of two ferrite HOM absorbers with step transitions to the beam tube, and by their asymmetric and significantly increased distances from the cavity ends. This geometry lowers the signal level at accessible ports but several dipole modes nevertheless have been identified via the comparison of the measured data with MWS simulations using the portable ferrite parameters. The room-temperature measurements performed on the string and the method at HOM identification are discussed in Sec. IV. The totality

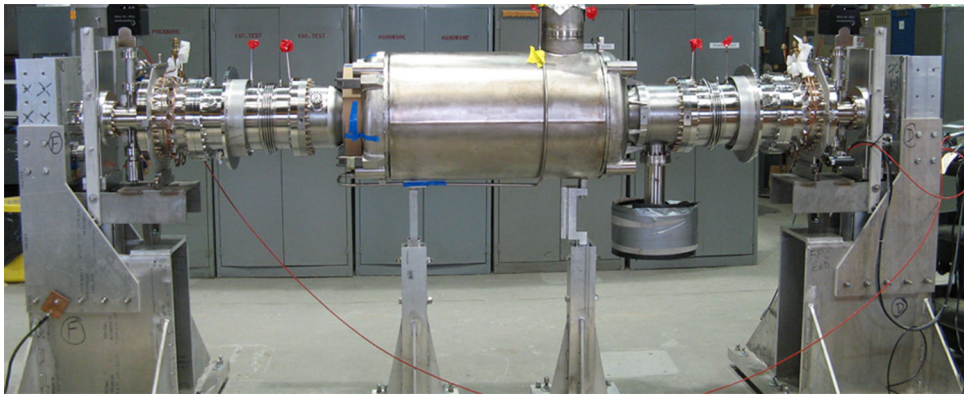

FIG. 1. (Color) The ERL cavity string.

of the results collected confirms the effective damping of HOM's in the ERL by the ferrite absorber and allows making credible projections of R/Q values and estimates of dipole shunt impedance values for use in beam dynamic studies.

II. PROTOTYPE CAVITY

Prior to the final design of the Nb cavity, a five-cell Cu prototype cavity was fabricated and methods of avoiding trapped HOMs were studied. Adding the prototype absorber to the Cu cavity and performing room-temperature measurements provided data for several critical HOMs and confirmed the suitability of the use of ferrite absorbers. The results for the bare cavity and the global absorber damping are presented in this section.

A. The bare copper cavity

The ERL cavity center cell is fabricated with a 41.874 cm equator, a 17.023 cm iris diameter, and a cell length of 21.331 cm at room temperature for cold operation at 703.75 MHz. The end cell is adjusted for field flatness and the cavity is connected to the HOM absorber by nominally 24 cm diameter beam tubes as seen in Fig. 2.

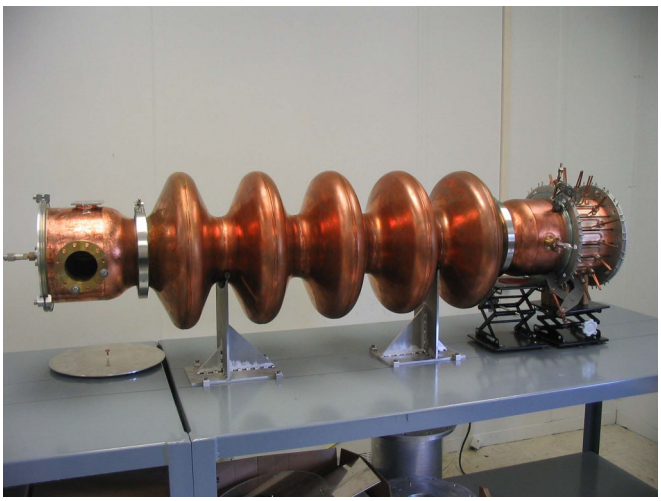

FIG. 2. (Color) The five-cell Cu cavity with prototype ferrite HOM absorber.

In preparation for the discussion of HOMs, a MWS model of the bare ERL cavity without absorber or beam tubes was constructed based on the detailed AES fabrication drawings. The relevant properties from the MWS simulation (indexed MWS) and the measured frequency values (indexed Data) for the bare Cu cavity (indexed Cu) are listed in Table I for the fundamental modes and for the lowest dipole modes in Table II.

The simulation model was tested against the fundamental modes in the prototype cavity, which due to the TM_{01} cutoff frequency of the beam tube are not affected by the

TABLE I. ERL cavity fundamental modes.

f_{Data} [MHz]	f_{MWS} [MHz]	R/Q_{MWS} [Ω]	Q_{Cu}
683.8	683.3	0.00	21 600
688.9	688.3	0.05	22 200
695.6	694.7	0.00	23 000
700.9	699.9	0.20	23 700
703.0	702.0	397.76	22 100

TABLE II. Dipole pass bands in the Cu cavity.

f_{Data} [MHz]	f_{MWS} [MHz]	Q_{Cu}	R/Q_{MWS} [Ω]
808.8	806.5	27 900	0.06
825.3	823.2	28 500	0.76
847.3	846.5	28 800	4.30
867.1	870.7	28 400	43.91
879.2	889.3	27 100	74.35
888.0	896.4	27 300	13.76
924.3	957.5	37 100	0.01
965.0	962.6	37 400	0.62
974.9	969.4	37 400	13.14
988.1	979.1	42 000	6.5
1001.3	993.3	50 400	0.1

presence of the absorber. A full agreement between data and simulation is prevented by differences in the cavity geometry as built and the simulation model, so that an agreement of better than ~0.1% cannot be expected. The measured Q data are all above ~10 000 but joint losses keep them below the MWS perturbation value for a copper cavity with $\sigma = 5.8 \times 10^7/\Omega\text{m}$, and measured Q values for the bare cavity need not be quoted. The measured frequencies and the MWS simulation results for the fundamental resonance group in the five-cell cavity are given in Table I.

The relevant properties from the MWS simulation for the lowest dipole modes in the bare cavity with shorted ends are listed in Table II. The two lowest pass bands, the TE_{11} (H_{11})-like modes in the 800 MHz range and the TM_{11} (E_{11})-like modes in the 900 MHz range, are clearly distinguishable. It is to be noted that the π mode is precluded in the TM_{11}-like pass band. Resonance frequencies and R/Q change when the absorber is added, but in spite of these limitations, the HOMs in the bare copper cavity are valuable input for mode identification in the ERL cavity with the beam tubes and absorber attached. To serve as reference, the R/Q "accelerator" values and the quality factors for the Cu cavity with $\sigma = 5.8 \times 10^7/\Omega\text{m}$ are also listed. The R/Q dipole values are obtained with the MWS eigenvalue solver program at a resonance, $k = \omega/c$, via the longitudinal R/Q at the radial position a, from which follows the transverse value in units of "Ohm" as

$$\left(\frac{R}{Q}\right)_\perp = \frac{1}{(ka)^2}\left(\frac{R}{Q}\right)_\parallel \tag{1}$$

or in the circular accelerator units "Ω/m" as

$$\left(\frac{R}{Q}\right)_\perp^{\Omega/\text{m}} = k\left(\frac{R}{Q}\right)_\perp^{\Omega}. \tag{2}$$

B. Global study of ferrite-damped HOMs

The damping properties of the ferrite were studied globally by determining the frequencies and quality factors of the HOMs in the Cu cavity with and without the absorber via S_{21} measurements with a network analyzer. For this, the cavity is excited by an input probe centered on the shorting disk on the left side in the picture, shown in Fig. 2. The output signal is taken either with a probe on the shorting disk on the right end, or at the cavity side with the pickup (PU) probe intended for rf operation of the Nb cavity. The pickup probe is sensitive to monopole as well as dipole modes, and, due to its close-by location, sees all cavity modes. The axially located probe at the end strongly favors monopole modes but is separated from the cavity by the beam tube with its ~24 cm diameter. The beam tube limits wave propagation of the monopole modes to the end probe below ~957 MHz, but allows propagation to the PU probe of hybrid dipole modes at frequencies above ~733 MHz.

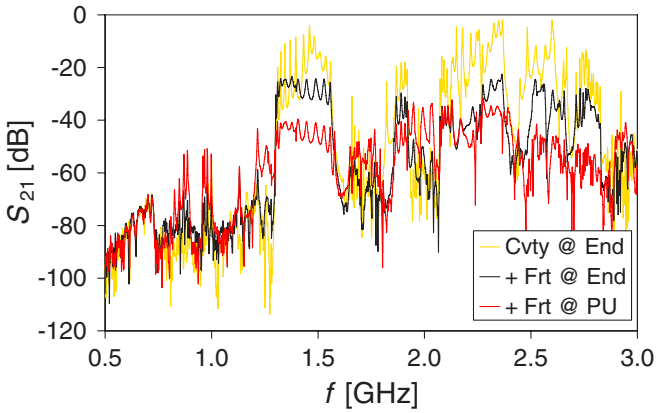

FIG. 3. (Color) S_{21} in Cu cavity without (yellow) and with (black and red) ferrite absorber.

For the measurements, the signal level is maximized by adjusting the input probe to achieve critical coupling for the fundamental cavity resonance at 703 MHz. The S_{21} transmission coefficients from input to the end and to the PU probes are shown in Fig. 3. In order to maintain the electrical length and node positions of the standing waves, the ferrite absorber is replaced by a beam tube of equal length for the state without ferrite. The output signal at the cavity end, yellow, shows (1) clearly the TM_{01} wave suppression by the beam tube below cutoff, (2) the strong damping by the absorber, black, and (3) the relative weak signal on axis of dipole modes, red. The Cu cavity tests provide a global confirmation of the effective damping of the HOM by the ferrite absorber. A more detailed study will be presented in the subsequent sections.

III. FERRITE ABSORBER

The production HOM absorber for the superconducting ERL cavity is a cylindrical spool with ferrite tiles soldered to 10W3 Elkonite plates at the wall, similar to the proto-

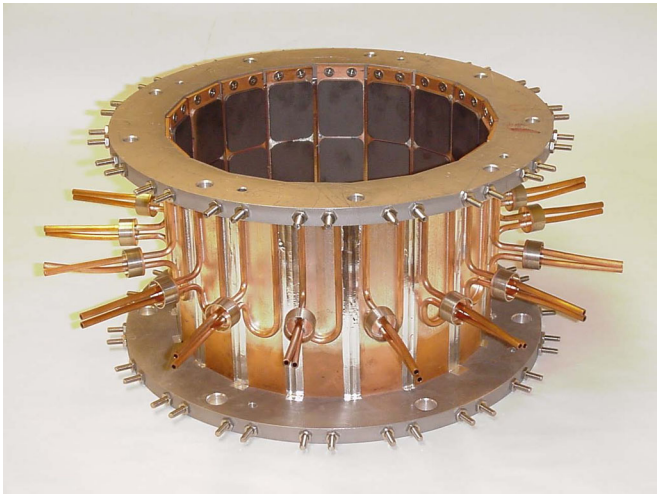

FIG. 4. (Color) HOM ferrite absorber prototype.

type model shown in Fig. 4. The unit has 18 plates in the 25 cm diameter spool, each with two tiles of ~24 cm dimensions. The production unit was designed and fabricated to withstand ~10 kW HOM load [15]. In normal operation of the ERL cavity, the absorber is at room temperature but can be water cooled through the tubes soldered to the plates. Completing the description of the absorber requires the knowledge of the microwave ferrite properties. Measuring the freestanding absorber properties was a necessary prerequisite for the study of the HOMs in the ERL.

The absorber and its MWS model are constructed as an assembly of many small ferrite tiles with interspersed gaps and exposed metallic stripes which, in the simulation program, requires large mesh sizes resulting in prohibitive running times. Therefore, a critical objective for the present study was finding portable absorber properties via parameters which describe the damping globally without the need of considering the tiled structure. Portability was obtained in the form of a ferrite cylinder with equivalent permeability and permittivity for use in simulation programs.

The use of microwave absorbing ceramic and ferrite materials is an important topic to various areas of technology and has previously been considered for the damping of HOMs at accelerator laboratories [16]. The absorbing material used here for the ERL absorber is a C48 ferrite [17] for which the room-temperature properties were measured by Mouris and Hutcheon (MH) at the Canadian Light Source (CLS) [18]. The MH data for complex microwave permeability and permittivity data of the C48 ferrite was obtained from measurements of small pellets, 3.5 mm in diameter and 3.175 mm thick at frequencies from 915 to 2800 MHz, covering the frequency range of interest to the present study. Although relevant, any effect due to the geometrical difference in the tiled absorber structure had to be determined on the prototype model for the purpose of this study.

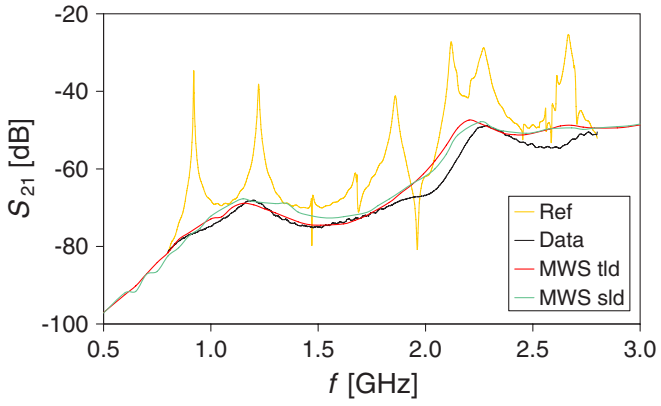

FIG. 5. (Color) Measured S_{21} for the absorber (Data) and a reference cavity (Ref) and curves simulated (MWS) with $\mu \approx 4(1 - j2.5)$ at 1 GHz and $\varepsilon \approx 13$.

A. Portable parameters from the ferrite absorber cavity

The approach taken here to find portable ferrite properties consists of transforming the prototype absorber into a ferrite-loaded pill-box with axially located probes for standard scattering coefficient measurements and their concomitant interpretation by simulation in the MWS program. The measured S_{21} coefficients for the absorber (Data) and a reference cavity (Ref) with the same geometry covering the frequency range from 0.8 to 2.8 GHz are shown in Fig. 5. The identifiable resonances of the reference cavity are TM_{01n} at 0.92, 1.22, and then TM_{02n} at 2.12, 2.28, 2.67 GHz, whereas the other visible resonances are attributed to dipole modes. The TM_{010} and TM_{020} resonance in the absorber are fully damped and the shallow peaks are at TM_{011} and TM_{021}.

The absorber data is compared with the MWS simulation results from a model with fully tiled ferrites (tld), shown in Fig. 6, and one with the ferrite represented by a 3.15 mm thick cylindrical tube of 10 cm length (sld). The ferrite parameters, $\mu = \mu' - j\mu''$, are entered into the MWS frequency domain solver program in the form of a Debye 1st order model (with constant tangent delta fit), given by the real part, μ' and the $\tan\delta = \mu''/\mu'$ defined at a specific frequency. The frequency dependence of $\mu = \mu'(1 - \tan\delta)$ is obtained in the program from the expression

$$\mu = \mu_\infty + \frac{\mu_0 - \mu_\infty}{1 + j\omega\tau} \tag{3}$$

together with the constraint that

$$\frac{d\tan\delta}{df} = 0 \tag{4}$$

at the defining frequency. It is noted that in the MWS simulation changing the material definition frequency, while maintaining the material parameters at this frequency constant, changes the μ and $\tan\delta$ values at other frequencies. For the ferrite permittivity only the real part of the MH value of $\varepsilon \approx 13(1 - j0.04)$ was retained.

Matching the S_{21} data measured in the absorber prototype against simulations obtained with variable μ' and $\tan\delta$ provided the approximate value of $\mu \approx 4(1 - j2.5)$

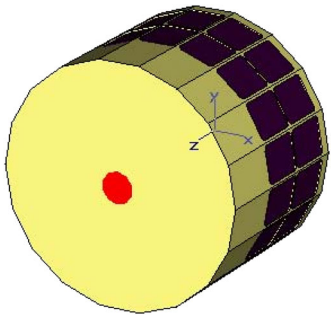

FIG. 6. (Color) MWS model of the prototype absorber with tiled bricks and axial port.

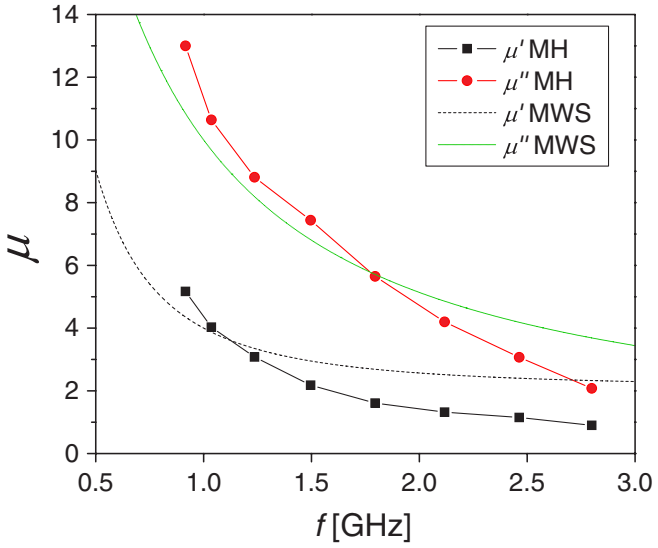

FIG. 7. (Color) Comparison of ferrite permeability $\mu \approx 4(1 - j2.5)$ used in the MWS simulations with MH results.

defined at 1 GHz for the MWS, or alternatively $\mu_0 \approx 55.93$, $\mu_\infty \approx 2.074$, and $\tau \approx 5.193$ ns for Eq. (3) over the frequency range from 0.8 to 1.6 GHz, which considering the electron bunch length of several mm in the ERL, is sufficient for the semiquantitative accuracy required for the HOM study in the ERL cavity.

B. Comparison with the Mouris and Hutcheon data

The ferrite permeability of the absorber has been found to be $\mu \approx 4(1 - j2.5)$, defined at 1 GHz, and will be applied over the frequency range from 0.8 to 1.6 GHz. It is to be noted that this portable approximation is in reasonable general agreement with the MH results as shown in Fig. 7. The small differences may be attributed to the underlying differences in geometries of pellets and tiles. It is possible that a more general permeability model could provide a better match, but finding it with and for MWS seems impractical and unnecessary.

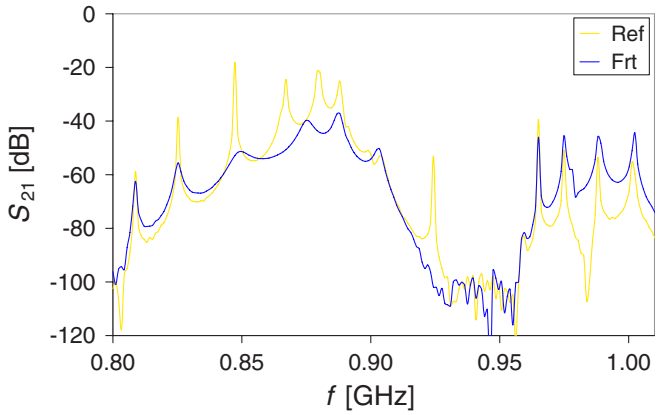

FIG. 8. (Color) HOM dipole modes in the five-cell Cu cavity without (Ref) and with (Frt) absorber.

C. Validation of portable ferrite parameters with the prototype cavity

Measuring the frequency and Q value of a cavity resonance is relatively accurate but finding the associated R/Q, although in principle possible with bead pulling, depends in practice on computer simulations with a valid model. The final test of the ferrite model and its parameters to be used for the ERL niobium cavity is performed by simulating the dipole modes in the five-cell Cu prototype cavity which is sufficiently complex to serve as a basis yet simple enough to develop a valid model. The S_{21} curves measured in the prototype cavity with either the ferrite absorber (Frt) or a copper tube of equal length (Ref) attached show the dipole HOM modes in Fig. 8.

Validation of the portable ferrite parameters is now obtained by considering the frequencies and quality factors of the dipole resonances in the prototype cavity. The measured and eigenvalue simulated results for the six TE_{11n} and the five TM_{11n} resonances are listed in Table III. It is worth noting that the resonance frequencies in the mid range of the table are changed by the presence of the absorber. Also listed is one of the additional reso-

TABLE III. Simulation of Cu cavity with tiled and solid absorber.

f_{Data} [MHz]	f_{tld} [MHz]	f_{sld} [MHz]	Q_{Data}	Q_{tld}	Q_{sld}	R/Q_{Cu} [Ω]	R/Q_{tld} [Ω]	R/Q_{sld} [Ω]	R_{tld} [Ω]	R_{sld} [Ω]
		802.3			1969			0.09		
808.8	808.4	820.3	1780	416	591	1.04	1.06	0.88	1887	1566
825.3	833.9	845.2	415	151	234	2.99	3.43	4.57	1423	1897
848.9	847.7	872.4	120	17	21	27.4	0.075	0.05	9	6
875.7	861.8	875.6	162	174	128	59.6	33.9	24.97	5492	4045
887.0	879.0	891.7	332	1599	1077	38.2	38.4	31.12	12 749	10 332
903.1	903.3	916.4	290	41.6	33	13.9	13.8	10.7	4002	3103
959.5	950.0	960.4	22 300	36 200	66 330	0.033	0.011	0.006	245	134
965.0	954.7	965.1	6670	7189	11 070	1.39	1.21	1.52	8071	10 138
974.9	962.1	971.8	2000	2766	4402	10.1	8.65	10.29	17 300	20 580
988.1	973.1	981.3	1064	1398	1978	3.43	3.38	3.40	3596	3618
1000.2	986.1	993.1	1512	1922	2701	1.06	1.09	1.17	1648	1769

nances, found in the simulation, which are located at the ferrite in the beam tube and which have low Q and very low R/Q values. It is worth noting that the resonance frequencies in the mid range of the table are changed by the presence of the absorber.

The first three columns in Table III compare the measured frequencies (indexed Data) with the simulated values for the tiled (indexed tld) and solid ring (indexed sld) models indicating agreement to better than ~2%. The Q values show only qualitative agreement between data and simulation; however, the tiled and solid model results are within a factor of 2, but do not favor either model. With the exception of one or two resonances, the R/Q values are in reasonable agreement, better than 30% between the tiled and solid ferrite models, again without favoring either model. In fact, mode identification in the case of closely spaced resonances is aided by R/Q matching. Overall, the results confirm that the tiled structure can be substituted with a solid ring without significant loss of accuracy. Furthermore, a practical rule for the interpretation of cavity tests towards finding the shunt impedance of a resonance consists in using the product of the measured Q data times the simulatedR/Q.

IV. ERL CAVITY

The five-cell SC ERL cavity, locally known as ''electron cooling xperimental'' (ECX), represents the center component of the energy-recovery linac at this laboratory. The design adopted nonstandard solutions, primarily in the exclusive use of ferrite dampers for a multicell cavity, and then the use of step transitions to reduce space requirements in multicavity cryostats. Evaluation of these concepts obviously depends on the completion of several steps, starting with the prototype cavity, the assembly of the ERL as the string shown in Fig. 1, cold emission tests, and acceleration test after the addition of the superconducting electron gun. The first definite results for the ERL have become available after the recent assembly of the niobium cavity as the string, reaching a critical milestone appropriate for recording of the results in this paper.

A. Absorber with step transition

The HOM damping depends on the magnetic field at the ferrite which suggested the possibility of enhancing the field with a metallic step at the absorber end. The prototype cavity was tested with the absorber end shorted and open, reflecting a step or in the latter case the presence of a taper. Table IV presents the measured frequency and Q values (subscript Data) as well as the MWS simulations for the shorted (superscript shrt) and ''waveguide'' terminated (superscript opn) model. Finding eigenvalues in the open model proved to be difficult and not all were found. The ~960 MHz resonance in all models has the character of a trapped mode, albeit with a very small shunt impedance. The measured and simulated results confirm that the additional Q-value damping from using a taper is either marginal or nonexistent, and the decisive benefit of a shorter cavity length in the ERL justified the adopted step transition at the absorber end. This is further supported by the mostly lower simulated R/Q values for the step transition.

B. ERL string tests

The ERL niobium cavity string, assembled with its beam position monitors, one pickup probe (PU), the fundamental power coupler (FPC), the two ferrite absorbers, and the closed vacuum gates allows already most measurements relevant to this paper which can be done without beam from the e-gun. The fundamental mode was measured between the FPC and the pickup probe (PU) in the cavity planned for the rf control system. The room-temperature frequency in the ERL cavity is found as 702.43 MHz with a $Q = 11\,000$. Cooldown will increase the frequency by ~1.035 MHz bringing it to 703.465 MHz which is within the slow-tuner range for the coherent electron cooling experiment at 703.5369 MHz.

The frequency range of interest to the HOMs covers the lowest dipole and monopole modes, from 0.8 to 1 and 1.2 to 1.6 GHz, respectively. The string is equipped additionally with three button probes (with Ceramaseal SMA feedthroughs) at both cavity ends which are intended for beam

TABLE IV. Measured and simulated results for the shorted and open prototype cavity.

$f^{\mathrm{shrt}}_{\mathrm{Data}}$ [MHz]	$f^{\mathrm{opn}}_{\mathrm{Data}}$ [MHz]	$Q^{\mathrm{shrt}}_{\mathrm{Data}}$	$Q^{\mathrm{opn}}_{\mathrm{Data}}$	$Q^{\mathrm{shrt}}_{\mathrm{MWS}}$	$Q^{\mathrm{opn}}_{\mathrm{MWS}}$	R/Q^{shrt} [Ω]	R/Q^{opn} [Ω]
808.8	808.8	1780	670	591	263	0.9	0.6
825.3	826.4	415	490	234	203	4.6	6.5
848.9	849.5	120	300	21		0.1	
875.7	873.7	162	211	128	326	25.0	44.6
887.0	886.9	332	275	1077	1849	31.1	38.8
903.1	901.2	290	730	33	73	10.7	15.1
959.5	959.5	22 300	12 160	66 330	72 224	0.0	0.0
965.0	965.0	6670	2815	11 070	10 171	1.5	1.3
974.9	974.9	2000	890	4402	3694	10.3	10.9
988.1	988.1	1064	586	1978	1263	3.4	3.8
1000.2	1001.3	1512	1033	2701	1271	1.2	1.2

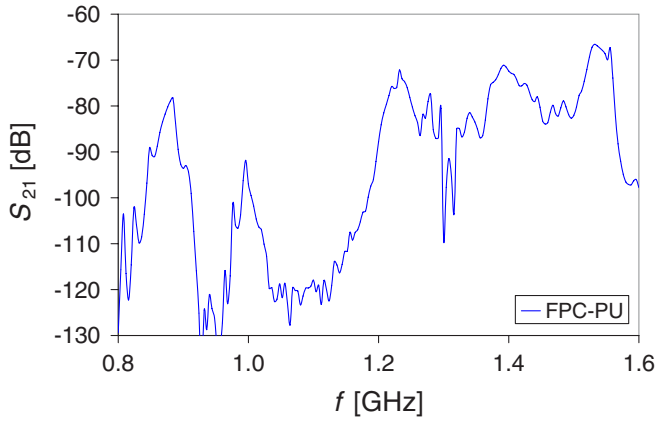

FIG. 9. (Color) S_{21} signal from FPC to PU in the ERL cavity.

position measurements but allow scattering coefficient measurements of HOMs. The buttons provide signals without regard to their polarity and are strong sources for dipole modes, but are not reached by the fundamental mode. The HOMs are studied via S_{21} measurements between the access points in several configurations, the one between FPC and PU is shown in Fig. 9. The resonances are all strongly damped and many resonances are overlapping, especially in the monopole range, nevertheless several individual Q values have been measured in the dipole range. Mode identification leading to shunt impedance values depends on finding the R/Q from MWS simulations with the Jacobi-Davidson method eigenmode solver. Because of the density of resonances in the ERL string, the MWS eigenmode solver failed to find results with lossy ferrite above $\sim$1 GHz and prevented a quantitative discussion of monopole modes.

C. Dipole HOMs

Several dipole modes at frequencies below 1 GHz were measured and could be identified by comparison with simulation results. Mode identification by comparing field distribution with the bare prototype cavity is prevented by the asymmetry of the ERL string and a strongly changed field pattern. Mode identification is aided by matching the simulated R/Q values for a Cu and a ferrite cavity of equal geometry. For this purpose, an exact, but still rotationally symmetric, ERL string model was generated from the bare Cu cavity by adding the beam tubes and both ferrite absorbers to assure equal basic geometrical dimensions. Two simulation runs were then made for which the ferrite was first treated as vacuum (subscript Cu) and then given by $\mu = 4(1 - j2.5)$ defined at 1 GHz (subscript Frt). The simulation results are listed in Table V and are also compared with measured data. The effect of the ferrite on the resonance frequencies is small, less than $\sim$0.5% in frequency, but slightly higher in the R/Q values.

The damping of the Q values by the ferrite absorbers is almost 2 orders of magnitude larger for the TE_{11}-like modes in the 800 MHz range but appears to be significantly lower for some of the TM_{11}-like modes in the 900 MHz range. The HOM shunt impedances in the SC ERL cavity are determined primarily by the absorber and thus are already given for the superconducting state by the present measurements. It is recalled here that trapped modes have been avoided by the "open" cavity design, although at least one mode, apparently with near zero R/Q, seems to remain undamped by the ferrite.

The R/Q values from the "vacuum" and ferrite simulation runs are largely determined by the cavity geometry and thus are in good numerical agreement. Using the method developed from the absorber study of the prototype in the previous section, shunt impedance values can be estimated by multiplying the measured Q data with the R/Q from simulation, both values with the ferrite absorber. If in the case of closely spaced resonances convergence to a simulated R/Q value is not achieved, the readily found results from lossless simulations can be substituted at the expense of a slightly reduced accuracy.

TABLE V. Dipole resonances in the ERL cavity.

f_{Cu} [MHz]	f_{Frt} [MHz]	f_{Data} [MHz]	R/Q_{Cu} [Ω]	R/Q_{Frt} [Ω]	Q_{Frt}	Q_{Data}	R_{Frt} [Ω]	R_{Data} [Ω]
805.1	803.4		0.04	0.13	588		76	
810.2	808.4	807.8	0.37	1.12	150	900	168	1008
817.9	816.1		1.18	0.73	136		99	
829.2	827.0	825.18	0.32	0.22	265	370	59	81
851.6	849.5	848.99	13.75	11.84	493	130	5839	1539
874.6	872.6		55.08	49.33	379		18 697	
890.2	888.1		43.02	42.01	163		6847	
897.1	895.0		21.19	22.78	201		4578	
929.0	926.2		10.12	6.66	104		693	
943.8	940.7		5.80	8.58	79		678	
957.6	956.1	958.34	0.05	0.04	40 370	9500	1571	380
963.7	962.2	964.76	2.64	2.65	6410	3350	16 977	8878
975.4	973.7	977.15	7.89	8.07	2132	830	17 210	6698
991.8	989.8	995.46	2.41	2.39	1644	205	3925	490

Several measured dipole modes have been identified by comparing the R/Q from MWS simulations of the string with and without the ferrite. Their shunt impedance values based on Q data and Q simulation are listed together in Table V. It is noted that the shunt impedance values derived from data are typically lower than the values from simulation with ferrite. Conservative estimates for all dipole shunt impedance values to be used in beam dynamics studies should thus be based on the simulation results obtained with the ferrite absorber.

In conclusion, the totality of the results confirms the effective damping of the dipole modes by the ferrite absorber in the ERL even in the case of a step termination. Furthermore, the MWS simulations of the ERL dipole modes allow making credible projections of R/Q values and estimates of dipole shunt impedance values for use in beam breakup and other beam dynamic studies.

ACKNOWLEDGMENTS

The authors would like to thank Dr. Ilan Ben-Zvi and Dr. Vladimir Litvinenko for helpful comments. The support provided by the Collider-Accelerator technical staff setting up the cavities was greatly appreciated. This work was supported by Brookhaven Science Associates, LLC under Contract No. DE-AC02-98CH10886 with the U.S. Department of Energy.

[1] I. Ben-Zvi, 13th International Workshop on RF Superconductivity 2007, Beijing, China (Report No. FR101), http://web5.pku.edu.cn/srf2007/proceeding.html.

[2] V. Litvinenko *et al.*, in *Proceedings of the 11th European Particle Accelerator Conference, Genoa, 2008* (EPS-AG, Genoa, Italy, 2008), p. 193.

[3] I. Ben-Zvi, in *Proceedings of the 2003 Particle Accelerator Conference, Portland, OR* (IEEE, New York, 2003), p. 39.

[4] R. Calaga *et al.*, BNL Collider-Accelerator Department Report No. C-AD/AP/111, 2003.

[5] R. Calaga, Ph.D. dissertation, SUNY Stony Brook, 2006).

[6] D. Moffat *et al.*, in *Proceedings of the 1991 IEEE Particle Accelerator Conference, San Francisco, CA* (IEEE, New York, 1991), p. 664.

[7] S. Belomestnykh *et al.*, in *Proceedings of the 1995 Particle Accelerator Conference, Dallas, TX* (IEEE, New York, 1995), p. 3394.

[8] T. Tajima *et al.*, in *Proceedings of the 1999 Particle Accelerator Conference, New York* (IEEE, New York, 1999), p. 440.

[9] Advanced Energy Systems, Medford, New York, NY 11763.

[10] ACCEL Instruments GmbH, 51429 Bergisch-Gladbach, Germany.

[11] CST-Computer Simulation Technology, Darmstadt, Germany.

[12] H. Hahn *et al.*, Physica (Amsterdam) **441C**, 239 (2006).

[13] H. Hahn *et al.*, BNL Report No. C-AD/AP/269, 2007.

[14] H. Hahn *et al.*, BNL Collider-Accelerator Department Report No. C-AD/AP/329, 2008.

[15] E. Chojnacki and W. J. Alton, *Proceedings of the 1999 Particle Accelerator Conference, New York* (IEEE, New York, 1999), p. 845.

[16] Proceedings of the First Workshop on Microwave-Absorbing Materials for Accelerators, CEBAF, Newport News, VA, 1993 (unpublished); I. E. Campisi, in *Proceedings of the Particle Accelerator Conference, Washington, DC, 1993* (IEEE, New York, 1993), p. 1115.

[17] Countis Laboratories, 12295 Charles Drive, Grass Valley, CA 95945.

[18] J. Mouris and R. M. Hutcheon, Canadian Light Source/ Microwave Properties North Report No. MPN-41-00, 2000.